Journal of Catalysis **201,** 70–79 (2001)
doi:10.1006/jcat.2001.3221, available online at http://www.idealibrary.com on IDEAL®

Studies on the Characterization of Several Iridium– and Rhodium–clay Catalysts and Their Activity in Imine Hydrogenation

Carmen Claver,* Elena Fernández,* Ramon Margalef-Català,* Francisco Medina,† Pilar Salagre,*,[1] and Jesus E. Sueiras†

*Departament de Química Física i Inorgànica, Universitat Rovira i Virgili, Pl. Imperial Tarraco 1, 43005 Tarragona, Spain; and †Escola Tècnica Superior d'Enginyeria Química, Universitat Rovira i Virgili, Pl. Imperial Tarraco 1, 43005 Tarragona, Spain

Received November 24, 2000; revised January 29, 2001; accepted March 6, 2001; published online May 24, 2001

Iridium– and rhodium–clay catalysts were prepared by immobilizing the complexes $[Ir(\mu\text{-}Cl)(COD)]_2$ [1] + $4PPh_3$, $[Ir(COD)(PPh_3)_2]BF_4$ [2], $[Ir(COD)(PPh_3)_2]PF_6$ [3], and $[Rh(COD)(PPh_3)_2]BF_4$ [4] in montmorillonite K-10 (MK-10), sodium bentonite (Na^+-MM), and lithium hectorite (Li^+-Hect). Other analogous supports were prepared after thermal and acidic modifications to montmorillonite K-10. For example, MK-10 was calcined at 500°C (MK-10-500) and treated with nitric acid ($H^+_{HNO_3}$-MK-10). The supports were characterized using XRD, BET surface area, FTIR, and acidity titration to confirm the properties of smectite–clay materials. The characterization of the immobilized iridium– and rhodium–clays was studied using XRD, FTIR, and conductimetric analyses. From these results, we found that the complexes are adsorbed mainly on the external surface of MK-10 and Li^+-Hect. However, the immobilization of the organometallic complexes on Na^+-MM is intercalated mainly by the ion-exchange process. Hydrogenation of the aldimine *N*-benzylidene aniline was studied with the iridium– and rhodium–clay catalytic systems. The aim of our study was to determine how the immobilized system influences the catalytic process, taking into account the metal, the counterion, and the acidity and composition of the support. In some catalytic systems the catalyst was reused for a significant number of consecutive runs. The catalyst 2–MK-10, for example, was reused in consecutive hydrogenations and showed high activity (>97% conversion) for at least 13 runs. The loss of catalytic activity as a consequence of the relative stability of the metallic intermediate species to air is also discussed.

Key Words: **montmorillonite; bentonite; hectorite; clay; hydrogenation of imines; iridium; rhodium; heterogenized; intercalation; adsorption.**

1. INTRODUCTION

The homogeneous catalytic hydrogenation of imines to amines (1–4), using metal transition complexes as catalytic precursors, is a well-known process that has attracted great attention in recent years, particularly in the asymmetric hydrogenation of prochiral imines (5–11). Although homogeneous catalysts can provide high conversion, most difficulties are encountered in separating the catalyst from the solution. Little effort has been made to separate the homogeneous catalyst from the products. Efficient catalytic hydrogenation of imines has been achieved with a two-phase system that uses a water-soluble catalyst (12–14), reverse micelles (15), zwitterionic complexes (16), and inorganic supports (silicates, semimetal or metal oxides, glass or mixtures) (17). However, to our knowledge, there have been no further studies into the recovery and reusability of the removable catalytic systems. Indeed, these properties might be ignored in a small-scale hydrogenation reaction in the laboratory, but they are very significant for the economic and technological viability of the large-scale production of amines. The presence of the metal catalyst could also cause problems with the purity of the product.

Immobilizing organometallic complexes in clay structures makes it possible to minimize many of the barriers associated with the unremovable homogeneous solution catalyst. Smectite clays such as montmorillonite and hectorite have recently attracted great interest as supports for heterogenized homogeneous catalysts because they combine cation exchange, intercalation, and swelling properties which make them unique (18, 19). From a catalytic standpoint, their ability to expand the interlamellar space is their most important property (18, 20).

In a previous study, we reported that the immobilization of the cationic iridium(I) complex $[Ir(COD)(PPh_3)_2]BF_4$ in montmorillonite K-10 hydrogenated the aldimine *N*-benzylidene aniline into the corresponding amine with the same conversion as the analogue homogeneous system. The heterogenized catalyst was indeed recovered and reused for 12 recycles with no apparent loss of activity (21). We observed that thermal and acidic modifications in the support negatively affect the stability of the active catalytic species,

[1] To whom correspondence should be addressed. Fax: +0034 977559563. E-mail: salagre@quimica.urv.es.

0021-9517/01 $35.00

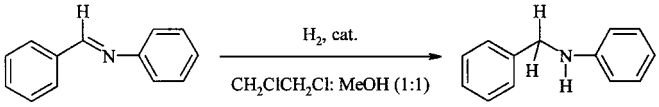

5 6

SCHEME 1

while modifications in the organometallic complex counterion decrease its stability.

To explore the potential of the immobilized catalytic systems, the present study discusses various factors that can influence the stability of the active species. In particular:

(i) the use of different type of smectite supports, such as sodium–bentonite, montmorillonite K-10 (dioctahedral smectites), and hectorite (trioctahedral smectite);

(ii) the use of cationic iridium(I) and rhodium(I) organometallic complexes, as well as neutral iridium complexes.

The hydrogenation of *N*-benzylidene aniline was chosen to test the catalytic activity of the immobilized systems (Scheme 1).

The organometallic complexes were characterized by elemental analysis, ^{1}H and ^{31}P NMR, and FTIR. The supports and the metal–clay systems were characterized by X-ray diffraction, BET surface area, FTIR, and acidity titration.

2. EXPERIMENTAL

2.1. Synthesis

All iridium and rhodium organometallic complexes were synthesized using standard Schlenk techniques under nitrogen atmosphere. All organic solvents were purified by usual methods, stored on a molecular sieve (0.4 nm, Aldrich), and degassed with a nitrogen flow before use. The complexes $[Ir(\mu\text{-Cl})(COD)]_2$ [**1**] (22), $[Ir(COD)(PPh_3)_2]X$ ($X = BF_4^-$ [**2**], PF_6^- [**3**]) (23, 24), and $[Rh(COD)(PPh_3)_2]BF_4$ [**4**], were prepared as previously reported (25). They were characterized by elemental analysis, ^{1}H and ^{31}P, NMR, and FTIR.

Montmorillonite K-10 (MK-10) was purchased from Fluka. Sodium montmorillonite (Na^+-MM) was obtained by purifying bentonite (BDH) as described by van Olphen (26).

$H^+_{HNO_3}$-montmorillonite ($H^+_{HNO_3}$-MK-10) was prepared from 10 g of MK-10 by treatment with 125 ml of saturated sodium chloride solution for 30 min. The solid was filtered under vacuum and treated with 125 ml of 0.1 N nitric acid solution for 1 h. The $H^+_{HNO_3}$-MK-10 was filtered, washed with water until the filtrate was nonacidic, and dried at 80°C (19).

$H^+_{NH_4NO_3}$-montmorillonite ($H^+_{NH_4NO_3}$-MK-10) was obtained as described in the literature (27). That is to say, 100 ml of an aqueous solution of 514 mg of NH_4NO_3 was added to a flask containing 10 g of MK-10. The solution was stirred at room temperature for 20 h. The solid was filtered, washed with water, and dried at 90°C. The dry solid was then finely pulverized and calcined at 500°C for 45 min to expel the ammonia.

Calcined montmorillonite, MK-10-400, and MK-10-500 were obtained as described below. MK-10 (5 g) was stored in a melting pot and kept in the oven at 400°C for 4 h or 500°C for 35 min.

Li^+-hectorite (Li^+-Hect) was synthesized in the following way (28). A 3% aqueous slurry containing silicic acid (1.58 g), magnesium hydroxide (0.6 g) (precipitated from a 25% solution of $MgCl_2 \cdot 6H_2O$ with 10 N ammonia, washed thoroughly, and homogenized), and lithium fluoride (92.3 mg) was made. The molar $SiO_2/Mg(OH)_2/LiF$ ratio was 4/3/1. The slurry was heated at 120°C in an oven in a locked Teflon flask for 15 days. The flask was cooled and the solid filtered under vacuum, washed thoroughly with water, and dried at 80–90°C.

The imine *N*-benzylidene aniline was prepared from aniline and benzaldehyde in ethanol medium as described in the literature (29). The imine was characterized by elemental analysis and ^{1}H and ^{13}C NMR.

The complexes were immobilized in the following manner. The dichloromethane solutions (10 ml) of each complex (0.1 mmol) (with the addition of triphenylphosphine (0.4 mmol) for the neutral complex) were prepared under nitrogen and added to a suspension of the solid support (MK-10, $H^+_{HNO_3}$-MK-10, Na^+-MM or Li^+-Hect) (1 g) in deoxygenated dichloromethane (10 ml), and then stirred for 24 h under nitrogen at room temperature. The suspension was filtered off and the solid washed with dichloromethane and dried under vacuum. The amount of metal complex immobilized on the clay was determined by gravimetric analysis. Conductimetric analyses of the filtrate were recorded to determine whether the interlamellar cation was replaced by the cationic complex and to what extent.

2.2. Hydrogenation Procedure

Hydrogenation experiments were carried out in a stainless-steel Berghof autoclave equipped with a magnetic stirrer at 40°C and 5 bar hydrogen pressure. The catalytic solution was contained in a glass vessel, and the inside of the autoclave's cap was coated with Teflon to prevent the solution from coming into direct contact with the stainless steel. In a standard homogeneous hydrogenation experiment, a solution of *N*-benzylidene aniline (2.5 mmol) in 1,2-dichloroethane:methanol (8 ml, 1 : 1) with catalyst precursor (0.05 mmol) was placed in the evacuated autoclave, heated, and stirred. For a heterogenized experiment the immobilized catalyst (0.05 mmol on metal) was introduced previously into the autoclave. Once the

systems had reached thermal equilibrium, hydrogen was introduced so that the working pressure could be reached. At the end of the reaction, the systems were cooled and the gas was vented. The reaction mixtures were analyzed by gas chromatography (previously filtered off for heterogenized systems). They were performed using a Hewlett–Packard 5890 II with a flame ionization detector in a *capillary* ULTRA-3 column with a content of 5% diphenylsilicone and 95% dimethylsilicone. The solid was washed with methanol and placed in the autoclave for a consecutive hydrogenation experiment.

2.3. Analysis Methods

Elemental analysis for C, H, and N of organometallic complexes was carried out on a Carlo-Erba microanalyzer.

IR spectra (range 4000–400 cm^{-1}) were recorded on a FTIR Prospect IR of Midac Corporation spectrometer in KBr pellets.

The effect of temperature on the structure and composition of the clays was monitored using FTIR. KBr pressed disks of the samples were prepared and treated at different temperatures and under different conditions. Those conditions were: (i) room temperature, (ii) vacuum at 120°C, (iii) calcination at 200°C for 1 h, (iv) calcination at 300°C for 1 h, (v) calcination at 400°C for 3 h, and (vi) calcination at 500°C for 3 h. After each calcination process, the disk was cooled under nitrogen flow to eliminate and prevent readsorption of water. The IR spectrum was recorded immediately. Nevertheless, in some cases, the disk was kept in contact with the air for 2 h and the spectrum was recorded to confirm the readsorption of water.

^{1}H and ^{31}P NMR spectra were recorded on a Varian Gemini spectrometer with a ^{1}H resonance frequency of 300 MHz, chemical shifts were reported relative to tetramethylsilane for ^{1}H and 85% H_3PO_4 for ^{31}P as the external reference.

X-Ray diffraction was used to determine the basal spacing and the swelling properties of the supports. The basal spacing of each sample was calculated from 001 reflection in its X-ray pattern. This basal spacing was associated with the distance between (001) layers (d_{001}) and was located at angles, 2θ, between 5° and 7°.

Powder X-ray diffraction (XRD) patterns of the different supports and catalysts were obtained with a Siemens D5000 diffractometer using nickel-filtered Cu$K\alpha$ radiation. XRD analyses of all samples were performed in thin films. These films were prepared by spreading a suspension of the sample in the swollen agent on a glass slide and drying the slide at room temperature or in an oven at 120°C for those analyses in which the basal spacing was studied. Due to this method, the plate-like particles presumably oriented themselves so that the 001 reflection was amplified to a greater extent than for the powder samples. Powder samples mounted on a glass microscope slide were also analyzed for support identification. The patterns were recorded for 2θ angles between 3° and 70°.

BET surface areas were calculated from nitrogen adsorption isotherms at 77 K using a Micromeritics ASAP 2000 surface analyzer and a value of 0.164 nm^2 for the cross section of the nitrogen molecule.

The acid treatment of the solid was carried out as follows: A charge of finely ground solid (≈2 g) was weighed on an analytical balance and transferred to a 100-ml Erlenmeyer flask, and 50 ml of 5% sodium chloride solution was added by pipet to the flask. The suspension was stirred at room temperature for 3 h. The solution was then decanted through a filter paper and the solid washed with the minimum amount of water until the washings were nonacidic. The filtrate was transferred to a volumetric flask. The amount of acid in the filtrate was determined by titration with 0.05 N sodium hydroxide solution, which had been standardized against potassium acid phthalate using phenophthalein as the indicator.

The solid acidity (mEq H^+/m^2) was calculated from the amount of solid in the filtrate. $[H^+]_{\text{filtrate}}$ was the concentration of acid measured in the filtrate; V was the volume of the volumetric flask; W_{solid} was the amount of solid used in the titration process; and A_{BET} was the BET surface area of the solid:

$$\frac{[H^+]_{\text{filtrate}}(\text{mEq } H^+/\text{liter}) \cdot V(\text{liters})}{W_{\text{solid}}(\text{g solid}) \times A_{\text{BET}}(m^2/\text{g})} = \text{mEq } H^+/m^2 \text{ solid} \quad [1]$$

Atomic absorption (graphite atomisation method) was registered on a Hitachi Z-8200 spectrophotometer equipped with a photomultiplier as the detector, a double-beam source, and a hollow-cathode iridium lamp (Teknokroma), using polarized Zeeman for noise correction. Both the $IrCl_3$ standards and the samples were treated with 65% nitric acid to make them soluble in water.

The conductivity of the washings in the intercalation processes was measured using a Micro CM 2201 Conductimeter (Crison), equipped with a conductivity cell with platinum plates and a glass body, and with an automatic compensatory temperature system which measures the temperature of the solution.

3. RESULTS AND DISCUSSION

3.1. Support Characterization

The X-ray patterns of the supports MK-10, Na^+-MM, and Li^+-Hect were compared with those in the JCPDS database. The supports MK-10 and Na^+-MM were identified as montmorillonite and Li^+-Hect as hectorite.

Three samples showed a characteristic peak associated with the 001 reflection (30), which varied between 12 and 15 Å. The width of this reflection in MK-10 and Li^+-Hect is wider than in the Na^+-MM X-ray diffractogram. This

TABLE 1

X-Ray Diffraction Data for the Supports: MK-10, Na^+-MM, and Li^+-Hect

	XRD analysis					
	d_{001} (Å)					
		Swelling solvent				
Support	Dried 120°	H_2O	Glycerin	CH_2Cl_2	Immobilization of **2** in CH_2Cl_2 medium	Collapsed T (°C)
MK-10	13.3	15.5	18.8	16	16.8	500
Na^+-MM	11.8	14.8	17.7	12.7	16	400–500
Li^+-Hect	13.0	15.0	18.8	13	13	300–400

may be due to the low crystallinity of MK-10 and Li^+-Hect, which was also confirmed by the BET surface area results (see below). Although both MK-10 and Na^+-MM are the same montmorillonite clay material, they showed significant differences in crystallinity. MK-10 is prepared from montmorillonite or bentonite by acid treatment (31). The acid activation process is severe enough to partially destroy the bentonite layer structure, so the clay particles become very disordered.

The powder X-ray diffraction data in Table 1 show the values for the basal distances of the supports after having been dried for 24 h at 120°C and also after the samples had been treated with different swelling agents, such as water, dichloromethane, and glycerin. The basal distances for total dehydrated clays are expected to be between 9.6 and 10 Å (18, 20, 32). In contrast, heating MK-10, Na^+-MM, and Li^+-Hect at 120°C for 24 h did not totally dehydrate the clays, because the basal distance observed was 11.8 Å for Na^+-MM, 13.3 Å for MK-10, and 13.0 Å for Li^+-Hect (Table 1). When the solids were treated with water, the basal distance increased to around 15 Å, as described in the literature (30). The smectites were totally dehydrated at temperatures between 300 and 500°C (Table 1). When montmorillonite MK-10 was heated from room temperature to 500°C, the X-ray diffractogram was recorded every 50°C. The 001 reflection peak moved from 15 Å to lower distances, which indicates that there was a progressive loss of interlamellar water until the collapsed basal distance (9.8 Å) was reached at 500°C. The dehydration process in Na^+-MM and the consequent collapse of the layers were progressive and were irreversible at temperatures above 400°C. The loss of ordered pillaring in the clay during the dehydration process was revealed by broadening of the peaks in the X-ray diffractogram. The basal distance of the completely dehydrated Li^+-Hect was 10 Å. Temperatures between 300 and 400°C were necessary for layers to collapse in the hectorite clay.

If the supports were exposed to different swelling agents such as CH_2Cl_2, H_2O, and glycerin, the basal spacing of the materials was higher than that of the initial dried clays. As expected for smectite-type materials, this observation indicates that the supports can intercalate solvents into their interlayer space and, thus, increase their basal distance. As reported in the literature (8, 30, 33), glycerin led to the greatest increase in the basal distance (5.5 Å for MK-10, 5.9 Å for Na^+-MM, and 5.8 for Li^+-Hect). The basal distance was similar for all solids when water was the swelling agent, but MK-10 showed a high value (16 Å) for dichloromethane. While Na^+-MM and Li^+-Hect have a greater affinity for water, MK-10 has a similar affinity for water and dichloromethane. This may be due to the partial loss of M^{3+} and M^{2+} cations, which modify the structure and composition of the material and, consequently, its solvent affinity. Both factors, the swelling properties of the MK-10 in dichloromethane and the complete solubility of the organometallic complexes in this solvent, make dichloromethane the solvent of choice for the immobilization process.

The BET surface area technique gives information about the structure of the pores and the area of the supports. All the supports characterized (MK-10, Na^+-MM, Li^+-Hect, MK-10-400, MK-10-500, $H^+_{HNO_3}$-MK-10 and $H^+_{NH_4NO_3}$-MK-10) were mesoporous materials (porous diameter around 45–58 Å). The values of the BET surface area are given in Table 2. When MK-10 was calcined at 400 and 500°C, the BET surface area values decreased slightly by about 10 m^2/g. The dehydroxylation processes, associated with the increase in temperature in the calcination process, modified the residual microporosity. This is observed mainly in the reduction of the microporous volume of the clay (5.5×10^{-3}, 2.6×10^{-3}, and 0.1×10^{-3} cm^3/g for MK-10, MK-10-400, and MK-10-500, respectively), which may explain the small variation in BET surface area. The surface area of Na^+-MM (49 m^2/g) was smaller than the surface area calculated for MK-10. Ravinchandran and Sivasankar (34) reported that the surface increased for acid-treated montmorillonite and that this increase depended on the acid concentration. However, the acid treatment has a limited capacity to increase the surface area. In this way, when MK-10 was again acidified with HNO_3 ($H^+_{HNO_3}$-MK-10) and NH_4NO_3 and then

TABLE 2

BET Area and Brønsted Acidity of the Clays Used as Supports for the Heterogenenization of Organometallic Complexes

Support	BET area (m^2/g)	Acidity (mEq H^+/m^2) $\times 10^{-4}$
MK-10	221	1.40
MK-10-500	211	1.27
MK-10-400	213	1.42
$H^+_{HNO_3}$–MK-10	215	7.69
$H^+_{(NH_4NO_3)}$–MK-10	213	4.33
Li^+-Hect	168	0
Na^+-MM	49	0

calcined ($H^+_{NH_4NO_3}$-MK-10), there was a slight reduction in the BET surface area of the solid. On the other hand, the high BET surface areas obtained for Li^+-Hect (168 m^2/g) are related to a badly constructed structure rather than to a structure that has been destroyed such as montmorillonite.

Table 2 lists acidity titration results as milliequivalents of H^+ per square meter (mEq H^+/m^2) of solid. The acidity value obtained was 1.4×10^{-4} mEq H^+/m^2 for MK-10 and for MK-10 calcined at 400°C (MK-10-400) and decreased slightly for MK-10-500 to 1.26 mEq H^+/m^2. The dehydroxylation of the acid surface observed in the IR study may explain these results (see below). In general, it was found that acidity values for characterized solids were much lower than those reported in the literature (35). This might be due to the fact that H^+ was not completely substituted by Na^+ from NaCl. Acidified MK-10 samples, $H^+_{HNO_3}$-MK-10 and $H^+_{NH_4NO_3}$-MK-10 have more Brønsted acid sites than the commercial MK-10. Their acidities were 7.7×10^{-4} and 4.3 mEq H^+/m^2, respectively. Thus, it seems that the subsequent acidification procedures did not increase the surface area of the solid but instead increased the number of Brønsted acid sites. Na^+-MM and Li^+-Hect have no Brønsted acidity. Low acidity was expected for both Na^+-MM and Li^+-Hect. Substitution with NaCl was used in the preparation of Na^+-MM and in Li^+-Hect; the acidity value is low because the hydroxyl concentration is low, as confirmed by the IR study (see below).

The IR spectra of smectite-type clays have two characteristic regions (36): (i) 4000–3000 cm^{-1} and (ii) 1200–400 cm^{-1}. The transmission bands in the first region, which correspond to ν(O–H), were assigned to the surface hydroxyl groups of the layer as well as to the adsorbed water. The bands in the region 1200 to 400 cm^{-1} are more informative about the structural characteristics of clay minerals and are attributed to lattice vibration (34, 36).

As stated above, MK-10 and Na^+-MM were identified as montmorillonite and Li^+-Hect as hectorite. Three solids presented characteristic structural sharp vibrations associated with the O–H stretching of hydroxyl groups ($\nu(O–H)_{OH} \approx 3630$ cm^{-1}) and vibrational broadbands of adsorbed water ($\nu(O–H)_{water} \approx 3450$ cm^{-1}). The stretching vibration of hydroxyl groups was significantly less intense in Li^+-Hect than in the other two solids. This indicates that there is only a low concentration of hydroxyl groups in the Li^+-Hect layers. This observation is in agreement with the literature (18, 36), which reports that some framework hydroxyls are replaced by fluoride ions from the LiF used in the preparation.

Figure 1 shows the IR spectra of the supports treated at different temperatures. In all cases, when the support was heated at 120°C under vacuum, we observed a considerable reduction in the intensity of the vibration bands, which was attributed to adsorbed water ($\nu(O–H)_{water}$ and δ(H–O–H)), although there was no significant difference

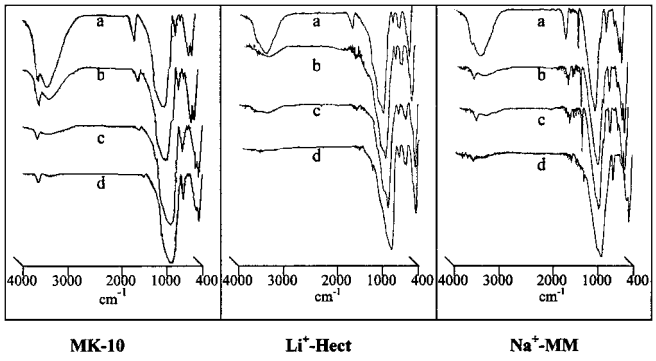

FIG. 1. IR spectra of MK-10, Li^+-Hect, and Na^+-MM clays at different temperatures: (a) room temperature; (b) vacuum and 120°C for 1 h; (c) 400°C for 3 h; (d) 500°C for 3 h.

in the other bands. However, at this temperature, the adsorbed water was not completely removed. The reduction in the intensity of the O–H stretching band of water enabled us to better see the bands associated with the hydroxyl group. Calcination of the samples at 200 or 300°C for 1 h considerably reduced the content of adsorbed water in the clay, although dehydroxylation processes were not observed. Calcining the solids at 400°C for 3 h significantly reduced the intensity of $\nu(O–H)_{OH}$. This indicates that dehydroxylation phenomena could have occurred. When the samples were calcined at 500°C for 3 h, water was completely removed and an important dehydroxylation process was observed. However, dehydroxylation was not completely accomplished at 500°C after 3 h in MK-10 and Na^+-MM. Only Li^+-Hect totally dehydroxylated, probably because of its low concentration of hydroxyl groups.

3.2. Ir– and Rh–Clay Characterization

The amount of metal complex $[Ir(\mu\text{-Cl})(COD)]_2$ [**1**] + 4PPh_3, $[Ir(COD)(PPh_3)_2]BF_4$ [**2**], $[Ir(COD)(PPh_3)_2]PF_6$ [**3**], and $[Rh(COD)(PPh_3)_2]BF_4$ [**4**] immobilized in MK-10, Na^+-MM, and Li^+-Hect was determined by gravimetric analysis (Table 3). These data suggest that the percentage of metal complex immobilized in the clay was higher when the metal species were cationic and the clay used as the support was MK-10 or Li^+-Hect. The neutral species (Table 3, entries 1, 7, 11) were present in the clay in lower concentrations than the cationic complexes. In all cases, the concentration of the immobilized complex was lower than that of the related systems described in the literature (80–100 mEq of complex per 100 mEq of clay) (31, 37, 38). This may be due to the partial destruction of the structure in the MK-10 and to the size of the complexes.

After the immobilization process, the new solids turned red (iridium complexes) or yellow (rhodium complexes). Thus, the presence of complexes in the support was established.

TABLE 3

Adsorbed Rhodium and Iridium Complexes in MK-10, MK-10-500, $H^+_{HNO_3}$-MK-10, Na^+-MM, and Li^+-Hect[a]

Entry	Immobilized complex	mmol complex/g
1	**1**–4PPh_3–MK-10	0.070
2	**2**–MK-10	0.081
3	**3**–MK-10	0.075
4	**4**–MK-10	0.076
5	**3**–MK-10-500	0.062
6	**3**–$H^+_{HNO_3}$-MK-10	0.074
7	**1**–4PPh_3–Na^+-MM	0.046
8	**2**–Na^+-MM	0.030
9	**3**–Na^+-MM	0.032
10	**4**–Na^+-MM	0.036
11	**1**–4PPh_3–Li^+-Hect	0.06
12	**2**–Li^+-Hect	0.073
13	**3**–Li^+-Hect	0.075
14	**4**–Li^+-Hect	0.074

[a] 0.1 mmol complex, 1 g of clay, and 10 ml of CH_2Cl_2 stirred at room temperature for 24 h under nitrogen.

IR spectra of Rh– and Ir–clay showed characteristic bands of the clay and a very low intensity band, around 3000 cm^{-1}, of COD vibrations (ν(C–H) and δ(C–H)). These IR spectra did not show vibration bands of PF_6^- or BF_4^-. However, we could not conclude that cation exchanges had taken place, because the clay vibration bands may have masked them. Thus, both cation exchange and the adsorption of the complex on the external surface were possible.

To determine whether the ion-exchange process had taken place, the solid immobilized species were filtered off and washed thoroughly with dichloromethane and water after the immobilization process. Conductimetric analysis and ^{31}P NMR of the liquid indicated that the interlamellar cations from MK-10 and Li^+-Hect were not replaced by the complex. In the case of the cationic complexes, the anionic counterions (PF_6^- and BF_4^-) were not present in the filtrates; they were presumably adsorbed on the support. When Na^+-MM was used as the support, conductimetric analyses of the washings revealed the presence of ionic species. This indicated that a cation-exchange process might have taken place. However, the replacement was not total and parts of the counterion and complex were adsorbed on the clay surface (Scheme 2). Low BET surface area clay values, in combination with the partial cation exchange, may explain the low concentration of the complex immobilized in Na^+-MM.

Powder X-ray diffraction of the supported systems showed the characteristic structure of lamellar clay. However, the diffractogram was broader than that of the original clay, indicating that the resulting systems were not as well ordered as the clays. When MK-10 and Li^+-Hect were used as supports for the immobilization process, the X-ray diffractogram of the heterogenized systems showed that the (001) diffraction line insignificantly shifted with respect to the clay swollen by CH_2Cl_2 (Table 1). The shift of (001) in the diffraction may be due largely to the intercalation of the dichloromethane used in the immobilization process. This, together with the results discussed above, indicates that the metal complex (cationic metal part and anionic counterion) was adsorbed mainly on the external surface of the clay when MK-10 or Li^+-Hect was used as support (Scheme 2). Crocker and Herold (31) reported the immobilization of $[Pd(PPh_3)_3(NCMe)][BF_4]_2$ in MK-10, which afforded higher concentrations of palladium on the surface than in the bulk. They observed that MK-10 tends to adsorb complexes on its surface and that its cation-exchange capacity is not high enough to intercalate the complexes between its layers. On the other hand, when Na^+-MM was used as the support, we observed a considerable increase in the basal distance of the clay when a metal complex was immobilized in it. The heterogenized system **2**–Na^+-MM presented a d_{001} of 16 Å, which means a Δd_{001} of 3.3 Å with respect to the clay swollen in dichloromethane (Table 1). This increase in the basal distance suggests that the complex has been intercalated between the silicate layers. However, the increase in the basal distance found in **2**–Na^+-MM is smaller than that reported in the literature for other complexes (37). The shift in the (001) diffraction was probably due only to one layer of the complex in the interlamellar space. These X-ray results together with the conductimetric analyses suggest that the organometallic complexes were partially intercalated between the layers in Na^+-MM by a cation-exchange process (Scheme 2), as described in the literature (39). It is assumed that iridium and rhodium complexes are taken up in a monolayer and that the square planer sheet of each complex is arrayed parallel to the silicate layer.

3.3. *Catalytic Hydrogenation*

The hydrogenation of *N*-benzylidene aniline [**5**] with $[Ir(\mu\text{-Cl})(COD)]_2$ [**1**] + 4PPh_3, $[Ir(COD)(PPh_3)_2]BF_4$ [**2**],

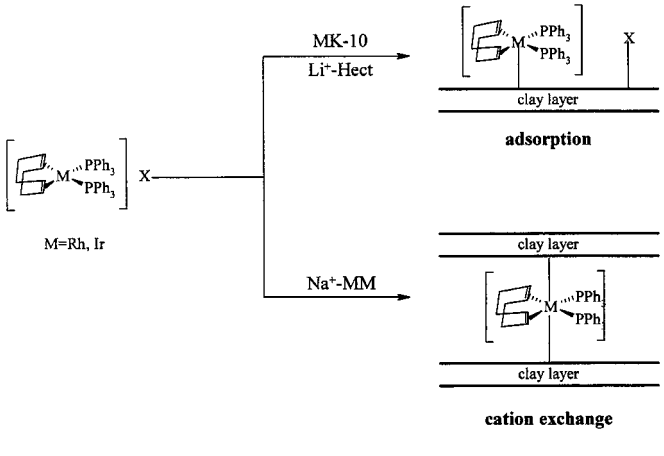

SCHEME 2

TABLE 4

***N*-Benzylidene Aniline Hydrogenation Catalyzed by Heterogenized Ir– and Rh–Clay Systems**[a]

Entry	Catalyst precursor	Run												
		1	2	3	4	5	6	7	8	9	10	11	12	13
		% Conversion												
1	**3**–MK-10	98	97	99	97	83	56	40	27					
2	**3**–MK-10-500	98	98	98	84	82	69	66	51					
3	**3**–$H^+_{HNO_3}$-MK-10	98	54	21										
4	**2**–MK-10	98	97	98	96	98	98	99	99	98	99	99	99	98
5	**1**–4PPh_3–MK-10	97	95	96	90	68	68	64						
6	**4**–MK-10	82	40	31	40									
7	**3**–Li^+-Hect	89	26	6										
8	**2**–Li^+-Hect	92	32	24										
9	**1**–4PPh_3–Li^+-Hect	9	1											
10	**4**–Li^+-Hect	85	28	12										
11	**3**–Na^+-MM	93	88	84	59	50	35							
12	**2**-Na^+-MM	90	86	80	74	75	69	68	60					
13	**1**–4PPh_3–Na^+-MM	55	52	55	73	74	75	73	74					
14	**4**–Na^+-MM	20	28	23	20									

[a] Standard conditions: *N*-benzylidene aniline, 4 mmol; catalyst precursor, 0.08 mmol M (M = Rh, Ir); solvent: $ClCH_2CH_2Cl$/MeOH (1 : 1), 8 ml; $P(H_2) = 5$ atm; $T = 40°C$; reaction time = 3 h.

$[Ir(COD)(PPh_3)_2]PF_6$ [**3**], and $[Rh(COD)(PPh_3)_2]BF_4$ [**4**] immobilized in MK-10, Na^+-MM, and Li^+-Hect, was carried out under standard condition ($ClCH_2CH_2Cl$/MeOH (1/1) as the solvent, 5 atm hydrogen pressure, 40°C, 3 h), to explore the possibilities of recovering the catalysts, the influence of the nature of the support, and the comparison of the activity and stability of supported catalysts and their homogeneous counterparts. Table 4 summarizes the catalytic results obtained when the metal species **1** + 4PPh_3, **2**, **3**, and **4** were immobilized on different supports, such as MK-10, MK-10-500, $H^+_{HNO_3}$-MK-10, Na^+-MM, and Li^+-Hect. The activity of the homogenous counterparts catalytic systems is shown in Table 5. In all cases, benzylphenylamine [**6**] was the only product of the reaction. Hydrolysis of **5** was not observed.

The results show that the homogeneous iridium systems, $[Ir(\mu\text{-}Cl)(COD)]_2$ + 4PPh_3, $[Ir(COD)(PPh_3)_2]BF_4$ and $[Ir(COD)(PPh_3)_2]PF_6$, lead to quantitative conversion of **5** to **6**, under the hydrogenation conditions. There were no significant differences in the electronic natures of the complexes. However, the rhodium catalytic precursor $[Rh(COD)(PPh_3)_2]BF_4$ decreased the catalytic activity (89%).

When the organometallic complexes were immobilized on the solid supports (MK-10, Na^+-MM, and Li^+-Hect), we observed that, in the first run, the catalytic activity of most of the heterogenized systems tested was similar to that of their homogeneous counterparts (>90%). However, when the heterogenized catalytic precursors **1**–4PPh_3–Li^+-Hect, **1**–4PPh_3–Na^+-MM, and **4**–Na^+-MM were used, the catalytic activity decreased dramatically with respect to their homogeneous counterparts. It should also be noted that, in the first run, there was a slightly larger reduction in the catalytic activity when Li^+-Hect and Na^+-MM were used as supports than when MK-10 was used (Table 4).

Table 6 shows the number of consecutive runs with conversion higher than 75% for the different heterogenized systems used. When the heterogenized cationic iridium systems were reused the conversion was above 75% for a larger number of consecutive runs than the other heterogenized systems with the same support. Using cationic iridium systems (**2** and **3**) heterogenized in MK-10 (**2**–MK-10 and **3**–MK-10), we observed that the catalyst deactivated at a different rate. Although **2**–MK-10 showed high activities (>97% conversion) for at least 13 consecutive runs (Table 4, entry 4), the analogous species **3**–MK-10 had a conversion lower than 75% after the fifth run (Table 4, entry 1). These results are in agreement with X-ray and conductivity studies and confirm that the counterion of the cationic iridium complex is also adsorbed into the

TABLE 5

***N*-Benzylidene Aniline Hydrogenation Catalyzed by Homogeneous Catalytic Systems**[a]

Entry	Catalyst precursor	% Conversion
1	**1** + 4PPh_3	96
2	**2**	99
3	**3**	99
4	**4**	89

[a] Standard conditions: *N*-benzylidene aniline, 4 mmol; catalyst precursor, 0.08 mmol M (M = Rh, Ir); solvent: $ClCH_2CH_2Cl$/MeOH (1/1), 8 ml; $P(H_2) = 5$ atm; $T = 40°C$, reaction time = 3 h.

TABLE 6

Number of Consecutive Runs in Hydrogenation of *N*-Benzylidene Aniline with Conversion Values on Amine >75%

	Complex			
Support	$1+4PPh_3$	2	3	4
MK-10	4	13[b]	5	1
Na^+-MM	5[a]	5	3	—
Li^+-Hect	—	1	1	1

[a] %C was smaller than 75% from the first to the third run. In the next five runs the %C reached values about 75%.

[b] All the %C values were >97.

montmorillonite. The presence of BF_4^- seems to make the heterogenized catalytic system much more stable; however, its influence in our catalytic process is not yet clear. It is known that the counterion of cationic organometallic complexes affects catalytic processes; for example, the counterion BPh_4^- has a negative effect on the catalytic activity of some hydrogenation processes (38, 40). The activity of the heterogenized catalyst precursor **3**–Li^+-Hect was only high in the first run (89%) (Table 4, entry 7), and decreased to 26% in the second run. The drop in catalytic activity with this system may be associated with the long contact with air during filtration due to the texture of the catalytic system and, therefore, to the modification of the active species. When Na^+-MM was used as the support, the heterogenized system **3**–Na^+-MM showed conversions higher than 75% for three consecutive runs.

As has been observed with cationic iridium complexes, the catalytic system was more efficient when the support used in the heterogenization of the neutral iridium species was MK-10. So, although the catalyst **1**–$4PPh_3$–MK-10 gave conversions higher than 70% for the first four runs (Table 6), the species **1**–$4PPh_3$–Li^+-Hect was almost inactive (Table 4, entry 8). The conversions for the catalytic system **1**–$4PPh_3$–Na^+-MM were lower than for **1**–$4PPh_3$–MK-10 during the first three runs, increased to about 75% after the fourth run, and remained constant thereafter (Table 4, entry 13). These results suggest that the activation time for this catalyst precursor is longer. However, the maximum conversion is lower than the maximum for **1**–$4PPh_3$–MK-10. Finally, we observed that the rhodium heterogenized systems showed lower activities than the iridium systems, and that the activity of these heterogenized rhodium systems decreased rapidly after the first run.

These results indicate that either the clays or the organometallic complexes have a considerable effect on the catalytic process, because of the stability of the active metallic species formed.

It is known that the presence of Brønsted acid sites, in both homogeneous and heterogenized catalysis, has some effect on the activity, selectivity, and enantioselectivity of some catalytic reactions such as the carbomethoxylation of ethylene (31, 41), the hydrogenation of terminal olefins (42), and the hydrogenation of imines (17, 43). The acid modifications in the support may also bring about different acid–base interactions between the complex and the support, which in turn may modify the stability of the active species. Table 7 shows how the acidity of the support affects the reuse of the catalytic system (showing a %C > 75%) and, as a result, how this catalyst system can affect the stability of the active species. The results seem to indicate that a larger number of Brønsted acid sites in the support (catalyst **3**–$H^+{}_{HNO3}$-MK-10) did not stabilize the active species and that the catalytic activity decreased considerably after the first run (Table 4, entry 3). However, the other supports (catalysts **3**–Li^+-Hect and **3**–Na^+-MM) did not stabilize the active species either. The catalysts with supports characterized by moderate Brønsted acidity (**3**–MK-10 and **3**–MK-10-500) were reused efficiently for at least five runs. Activity was maintained and conversions were higher than 75%. However, in **3**–MK-10-500, the loss of activity after the fifth run was slower than in **3**–MK-10 (Table 4, entries 1 and 2).

The loss of activity that was observed when catalytic heterogenized systems were used may be associated with the progressive leaching of the iridium complex from the solid, but the amount of iridium found by atomic absorption analysis of the filtrate in the heterogenized hydrogenation reaction was negligible. The color of the solid changed only slightly after the first run. This fact and the observed increase in the enantioselectivity in its reuse, when immobilized iridium and rhodium complexes were modified with chiral ligands such as BDPP, confirm the presence of a complex in the solid (44). Thus, the loss of activity may be due largely to the modification of the active species after exposure to air. To confirm this hypothesis, we carried out an experiment that consisted of simulating six consecutive runs using the catalyst **3**–MK-10. The autoclave was not opened between each run and the amount of imine **5** for one run (4 mmol) was injected every 3 h. In this experiment, the conversion of imine **5** to amine **6** after 18 h (corresponding to six runs of 3 h each) was quantitative, in contrast to the

TABLE 7

Influence of the Acidity of the Supports on the Number of Consecutive Runs in Hydrogenation of *N*-Benzylidene Aniline with Conversion Values on Amine >75%

Catalyst	No. of runs	Acidity (mEq H^+/m^2) $\times 10^{-4}$
3–MK-10	5	1.40
3–MK-10-500	5	1.27
3–$H^+_{HNO_3}$-MK-10	1	7.69
3–Li^+-Hect	1	0
3–Na^+-MM	3	0

observed conversion of **3**–MK-10 (56%) after the sixth run when the autoclave was opened and the catalyst filtered off after each run. This result suggests that the active species is highly sensitive to air. The experiment also confirms that the immobilization of iridium(I) complexes in montmorillonite avoids the complex oligomerization responsible for the deactivation of the active species in homogeneous catalytic hydrogenation, as reported by Crabtree (45). Crocker and Herold (38) also reported that the immobilization of the complex means that the metallic centers are separated from each other.

As far as the formation of the hydride catalytic species and the reusability of the metal complex are concerned, when complex $[Ir(COD)(PPh_3)_2]PF_6$ was immobilized in MK-10 and MK-10-500 the catalytic activity in the hydrogenation of **5** was high in the first run and was maintained in consecutive runs to a greater extent than for other catalytic systems (Tables 4–6). The different behaviour observed in the reusability of these heterogenized systems might be related to the ability of the metal species to carry out oxidative addition with H_2 rather than O_2. It is known that low-valence d^8 complexes, such as iridium(I), are capable of undergoing oxidative addition (46). However, Crabtree reported that the capacity to oxidize iridium(I) complexes is a function of the Lewis acidity of the metallic center (45). The systems that present a major electron deficiency will be able to undergo oxidative addition only with species such as H_2 via an ionic mechanism and will be protected from the addition of more oxidizing agents such as O_2. When complex **3** is immobilized in montmorillonite, the interactions of the metal with the support might increase the electron deficiency on the metal. However, the low capacity for hydrogenating **5** from the heterogenized system, **1**–4PPh_3-Li^+-Hect, might be due to an oxidant interaction of the metallic species with the F^- of the support and/or the Cl^- from the starting organometallic complex, which may inhibit the formation of the hydride catalytic species. In general, both the formation and the stability of the active species might be a function of the electron density of the metal and, therefore, of the nature of the support site to which the complex is linked. Thus, low basic sites may transfer a smaller electron density and a stronger resistance to the oxidation of the active species. The smectite MK-10 is, in fact, a clay with weak Brønsted acid sites (O^--H^+) (47). These acid sites may act as a link to the complex with small donor capacities and may prevent the systems from oxidizing.

In conclusion, of all the immobilized organometallic complexes studied, $[Ir(COD)(PPh_3)_2]BF_4$ led to the most stable system. The best support for this immobilized complex was usually MK-10, although the immobilization of **1**–4PPh_3 in Na^+-MM afforded a catalytic system that, after a long period of induction, became very stable and showed a conversion of about 74%.

4. CONCLUSIONS

This study concentrated on the characterization of smectite-type clays, which were used to heterogenize organometallic complexes for the catalytic heterogenized hydrogenation of imines.

Complexes of the type $[M(COD)(PPh_3)_2]X$ (where M = Rh and Ir) were heterogenized in the smectite clay materials. The characterization studies of the heterogenization process and of the heterogenized systems showed that complexes are adsorbed mainly on the external surface of MK-10 and Li^+-Hect. However, in the case of Na^+-MM, the complexes are immobilized largely on the support by a cation-exchange process and intercalated between the silicate layers of the solid.

The application of Rh(I) and Ir(I) heterogenized systems in the hydrogenation of the imine *N*-benzylidene aniline was studied. The results showed that the activities in the first run of the heterogenized systems using different supports are comparable to those of their homogeneous counterparts. The activity of both homogeneous and heterogeneous systems showed that the iridium(I) cationic systems $[Ir(COD)(PPh_3)_2]X$ ($X = PF_6^-$, BF_4^-) represent the best catalytic activity. As far as the supports are concerned, the presence of F^- in a solid, such as Li^+-Hect, may inhibit the formation of the active species or prevent it from being reused. In general, the catalytic activity of the immobilized systems decreased when the solid catalysts were reused. This reduction is due to the presence of intermediate species, which may be oxidized by oxygen when they are exposed to air during the filtration step of the process. However, immobilizing the organometallic complex $[Ir(COD)(PPh_3)_2]BF_4$ in the supports studied afforded catalytic systems that could be reused for a large number of runs, with negligible loss of the catalytic activity. At the same time, we observed that the same metallic species heterogenized in different supports behaved differently. Our results show that the nature of the counterion of the complex, together with the acid and structural characteristics of the clay, plays an important role in the stability of the catalysts.

ACKNOWLEDGMENTS

This research was supported by DGES PB-97-0407-C05-01 and Generalitat de Catalunya (DGR) (Grant 1998FI 00782).

REFERENCES

1. Spindler, F., and Blaser, H. U., *in* "Transition Metals for Organic Synthesis" (M. Beller and C. Bolm, Eds.), Vol. 2. p. 69. VCH, Weinheim, 1998.
2. Blaser, H.-U., and Spindler, F., *in* "Comprehensive Asymmetric Catalysis" (E. N. Jacobsen, A. Pfaltz, and H. Yamamoto, Eds.), Vol. I. p. 247. Springer-Verlag, Berlin, 1999.
3. Kobayashi, S., and Ishitami, H., *Chem. Rev.* **99**, 1069 (1999).

4. James, B. R., *Catal. Today* **37**, 209 (1997).
5. Taravov, V. J., Kadyrov, R., Riermer, T. H., Holz, J., and Borner, A., *Tetrahedron: Asymmetry* **10**, 4009 (1999).
6. Cahill, J. P., Lighfoot, A. P., Goddard, R., Rust, J., and Guiry, P. J., *Tetrahedron: Asymmetry* **9**, 4307 (1999).
7. Willughby, C. A., and Buchwald, S. L., *J. Am. Chem. Soc.* **116**, 8952 (1994).
8. Tani, K., Onouchi, J., Yamagata, T., and Kataoka, Y., *Chem. Lett.* 955 (1995).
9. Sablong, R., and Osborn, J. A., *Tetrahedron: Asymmetry* **7**, 3059 (1996).
10. Sablong, R., Osborn, J. A., and Faller, J. W., *J. Organomet. Chem.* **527**, 65 (1997).
11. Zhu, G., and Zhang, X., *Tetrahedron: Asymmetry* **9**, 2415 (1998).
12. Bakos, J., Orosz, A., Heil, B., Laghmari, M., Lhoste, P., and Sinou, D., *J. Chem. Soc. Chem. Commun.* 1684 (1991).
13. Bakos, J.,"Aqueous Organometallic Chemistry and Catalysis," Vol. 3: "High Technology," NATO ASI Services 15, p. 231 (1994).
14. Lensink, C., and deVries, J. G., *Tetrahedron: Asymmetry* **3**, 235 (1992).
15. Buriak, J. M., and Osborn, J. A., *Organometallics* **15**, 3161 (1996).
16. Zhou, Z., James, B. R., and Alper, H., *Organometallics* **14**, 4209 (1995).
17. Pugin, B., (1997), WO 97/02232, Ciba–Geigy AG.
18. Pinnavaia, T. J., *Science* **220**, 365 (1983).
19. Choudary, B. M., Vasantha, G., Sharma, M., and Bharathi, P., *Angew. Chem. Int. Ed. Engl.* **28**, 465 (1989).
20. Pinnavaia, T. J., Raythatha, R., Lee, J. G. S., Halloran, L. J., and Hoffman, J., *J. Am. Chem. Soc.* **101**, 6891 (1979).
21. Margalef-Català, R., Salagre, P., Fernández, E., and Claver, C., *Catal. Lett.* **60**, 121 (1999).
22. Winkhaus, G., and Singer, H., *Chem. Ber.* **99**, 3610 (1966).
23. Green, M., Kuc, S. H., and Taylor, S. H., *J. Chem. Soc. A* 2334 (1971).
24. Chaloner, P. A., Hitchcok, P. B., and Reisinger, M., *Acta Crystallogr. Sect. C* **48**, 735 (1992).
25. Haimes, L. M., *Inorg. Chem.* **9**, 1517 (1970).
26. Van Olphen, H., *in* "An Introduction to Clay Colloid Chemistry," 2nd ed., p. 249. Wiley–Interscience, New York, 1977.
27. McCabe, R. W., *in* "Inorganic Materials" (D. W. Bruce and D. O'Hare, Eds.), p. 303. Wiley, Chichester, 1992.
28. Baird, T., Cairns-Smith, A. G., and MacKenzie, D. W., *Clay Miner.* **10**, 17 (1973).
29. Bigelow, L. A., and Eatong, H., "Org. Synth. Coll," Vol. I, p. 80. 1941.
30. MacEwan, D. M. C., *in* "The X-Ray Identification and Crystal Structures of Clay Minerals" (G. Brown, Ed.), pp. 143–207. Mineralogical Soc. (Clays Minerals Group), London, 1961.
31. Crocker, M., and Herold, R. H. M., *J. Mol. Catal.* **70**, 209 (1991).
32. Laszlo, P., *Science* **235**, 1473 (1987).
33. Moore, D. M., and Reynolds, R. C., Jr., "X-Ray Diffraction and the Identification and Analysis of Clay Minerals." Oxford Univ. Press, Oxford, 1989.
34. Ravinchandran, J., and Sivasankar, B., *Clays Clay Miner.* **45**, 854 (1997).
35. Vaccari, A., *Appl. Clay Sci.* **14**, 161 (1999).
36. Farmer, V. C., "The Infrared Spectra of Minerals," Ch. 15, pp. 331–363. Mineralogical Soc., London, 1974.
37. Chin, C. S., Lee, B., Yoo, I., and Kwon, T., *J. Chem. Soc. Dalton Trans.* 581 (1993).
38. Crocker, M., and Herold, R. H. M., *Catal. Lett.* **18**, 243 (1993).
39. Sento, T., Shimazu, S., Ichikuni, N., and Uematsu, T., *J. Mol. Catal. A* **137**, 263 (1999).
40. Schrock, R. R., and Osborn, J. A., *Inorg. Chem.* **9**, 2339 (1970).
41. Waller, F. J., *Br. Polym. J.* **16**, 239 (1984).
42. Schrock, R. R., and Osborn, J. A., *J. Am. Chem. Soc.* **98**, 2134 (1976).
43. Minato, M., Fujiwara, Y., and Ito, T., *Chem. Lett.* 647 (1995).
44. Margalef-Català, R., Claver, C., Salagre, P., and Fernández, E., *Tetrahedron: Asymmetry* **11**, 1469 (2000).
45. Crabtree, R. H., *Acc. Chem. Res.* **12**, 331 (1979).
46. Vaska, L., *Acc. Chem. Res.* **1**, 335 (1968).
47. Castillón, S., Claver, C., Fernández, E., Salagre, P., Serra, M., and Uriz, P., Repsol, P200001396, REPSOL-YPF (2000).